ARTICLES

Collisional Deactivation of $PH_2(\tilde{A}^2A_1;\ v'_2 = 1,0)$ and $PH_2(\tilde{X}^2B_1;\ v''_2 = 1)$ by Some Triatomic Molecules

Chieu Nguyen Xuan* and Alessandro Margani

Istituto di Metodologie Inorganiche e dei Plasmi, Consiglio Nazionale delle Ricerche, Area della Ricerca di Roma 1, Via Salaria Km 29.3, 00016 Monterotondo Scalo, Rome, Italy

Received: August 16, 2001; In Final Form: January 31, 2002

The deactivation constants of $PH_2(\tilde{A}^2A_1;\ v'_2 = 1,0)$ and $PH_2(\tilde{X}^2B_1;\ v''_2 = 1)$ which are due to collisions with CO_2, N_2O, and SO_2 have been measured. Comparisons with data due to rare gas and diatomic quenchers have shown that the electronically excited PH_2 species are probably quenched by multiple channel mechanisms of both physical and chemical nature for SO_2 and of prevalently physical nature for CO_2 and N_2O. A V−V energy transfer is clearly responsible for the vibrational relaxation of $PH_2(\tilde{X}^2B_1;\ v''_2 = 1)$ by these triatomic quenchers.

I. Introduction

Interactions of the PH_2 radicals in the $\tilde{A}^2A_1$ first excited and $\tilde{X}^2B_1$ ground electronic states with rare gases and a certain number of molecules have been investigated from both physical and chemical points of view in our laboratory.[1,2] Vibrational levels $v = 1$ and 0 of the bending mode of these species have been considered.

It has been seen that quenching of $PH_2(\tilde{A}^2A_1,v'_2)$ by the rare gases should occur through a collision-induced crossing to the isoenergetic underlying higher vibrational levels of the ground electronic state followed by a fast vibrational relaxation.[3]

As the variation of the relaxation probability of $PH_2(\tilde{X}^2B_1;\ v''_2 = 1)$ with rare gas quenchers does not follow the SSH (Schwartz, Slawsky, Herzfeld[4]) mass law, the deactivation should not be due to a simple V−T process, which was supposed to be operative at first sight. An intramolecular V−R,T mechanism that is due to the low moment of inertia of the hydrogen-containing PH_2 radicals should then be responsible for their removal.[3]

With the exception of the PH_3 molecule in self-quenching studies,[4] the molecular quenchers so far taken into consideration have been some diatomic molecules and in particular H_2, N_2, O_2, CO, and NO.[1] The mechanism of interaction with the PH_2 species in both excited and ground electronic states has been seen to be different for each of them.

With the experimental technique employed which consisted in generating the PH_2 radicals by photolysis of PH_3 with an ArF excimer laser, O_2 seemed to be involved in a chain reaction,[6] and its effect on PH_2 could not be studied. This chain reaction was also observed by Melville[7] and by Norrish and Oldershaw,[8] who put forward a mechanism where the reaction between PH_2 and O_2 acts as one of the chain-carrying reactions.

The interaction of NO with PH_2 in the ground electronic state is particularly interesting. Whereas $PH_2(\tilde{X}^2B_1;\ v''_2 = 0)$ is almost chemically unreactive with NO ($k = 5.47 \times 10^{-14}$ cm^3 molec.$^{-1}$ s^{-1}), the reaction constant of the ($v''_2 = 1$) species is larger by a factor of 122 ($k = 6.68 \times 10^{-12}$ cm^3 molec.$^{-1}$ s^{-1}), and a mechanism has been proposed to explain this enhancement.[2]

So far, this is all that is known about the chemical reactivity of PH_2. As PH_3 has been recognized to be an important component of the photochemistry of the atmospheres of Jupiter and Saturn,[9] and of the chemical vapor deposition processes for the manufacturing of semiconductors,[10] PH_2 must also play an important role in the elementary reactions which underlie these systems. It should thus be useful to know more about the dynamics and reactivity of the excited and ground species of the PH_2 radicals in the presence of added molecules of more complex nature.

To be able to make comparisons with the data already gathered in previous papers and hopefully to derive new information about the interaction processes, we investigate in this work the effects of collisions, on the PH_2 species, of triatomic molecules, i.e. molecules one step higher in complexity than the so far studied diatomic ones, and in particular of N_2O, CO_2, and SO_2. NO_2 was included in the original plan of this work, but preliminary measurements have shown that the experimental technique used is unsuitable as NO_2 is excited by the same excitation wavelengths as PH_2.

The discussion of the new data will inevitably involve the revisiting and reformulating of the discussion of those reported in previous papers.

II. Experimental Section

The technique used to carry out the measurements was PH_3 photolysis by an ArF excimer laser combined with laser induced fluorescence (LIF) for the detection of the PH_2 species.

The experimental setup has been described in detail in previous papers;[1,2] therefore, the characteristics of the apparatus are only briefly outlined in the following.

The interactions of $PH_2(\tilde{A}^2A_1;\ v'_2)$ and $PH_2(\tilde{X}^2B_1;\ v''_2)$ with added molecules occurred in a black anodized alluminium

* Author to whom correspondence should be addressed. E-mail: Chieu.NguyenXuan@mlib.cnr.it.

10.1021/jp013181f CCC: $22.00
Published on Web 05/04/2002

reaction cell provided with lateral arms for the entrance and exit of the lasers.

A Lambda Physik model EMG 150 TMSC ArF laser with an average energy of 6−7 mJ/pulse was used to photolyze the PH_3 molecule and generate PH_2 species.

PH_2 fluorescence was induced by a Quanta Ray model PDL1 dye laser pumped by a Quanta Ray Model DCR1A Nd:YAG laser.

Fluorescence decay of $PH_2(\tilde{A}^2A_1;\ v'_2 = 0)$ and variation of $(\tilde{X}^2B_1;\ v''_2 = 0)$ concentrations were studied through excitation of the $^RQ_0(7_{17}\text{-}7_{07}$ and $4_{14}\text{-}4_{04})$ rotational transitions of $PH_2(\tilde{A}^2A_1;\ v'_2 = 0-\tilde{X}^2B_1;\ v''_2 = 0)$ system by 546.81 nm laser wavelength, whereas the $(\tilde{A}^2A_1;\ v'_2 = 1)$ and $(\tilde{X}^2B_1;\ v''_2 = 1)$ species were monitored exciting the $^RQ_0(6_{16}\text{-}6_{06}$ and $4_{14}\text{-}4_{04})$ transitions of $PH_2(\tilde{A}^2A_1;\ v'_2 = 1-\tilde{X}^2B_1;\ v''_2 = 1)$ band with 551.33 nm radiation.

The two laser beams were at right angles to each other, and the fluorescence signals were viewed and collected by a Thorn Emi 9816QB photomultiplier perpendicularly to both of them through, in the case of $PH_2(\tilde{A}^2A_1;\ v'_2 = 0)$ fluorescence, a system made up of a condensing lens of 150 mm focal length and a Schott OG 590 color filter which transmits the $(v'_2 = 0-\tilde{X}^2B_1;\ v''_2 \geq 1)$ bands and through an Oriel model 77250 1/8 m monochromator set to transmit only the $(v'_2 = 1 \rightarrow v''_2 = 2)$ emission in the case of $(\tilde{A}^2A_1;\ v'_2 = 1)$ fluorescence.

The photomultiplier output was then processed by a Tektronix model 7912AD transient digitizer. To study the quenching of $(\tilde{A}^2A_1;\ v'_2)$ species, the fluorescence decay curves were time analyzed, whereas for monitoring $(\tilde{X}^2B_1;\ v''_2)$ concentration variation during a reaction, the total fluorescence was collected at different delays from the photolysis flash.

The whole apparatus including the laser triggering system was under computer control.

All experiments were performed at room temperature (298 K).

Mixtures of PH_3, added gases, and Ar buffer gas were supplied to the reaction cell in a slow flow regime by a combination of MKS models 147, 250, and 1259 pressure and flow controllers provided with pressure feedback from capacitance manometers. Partial pressures of 0.1 Torr of PH_3 and 1 Torr of Ar were used in all experiments.

In view of the high toxicity of PH_3, the whole apparatus, gas manifold, reaction cell, pump connections, etc., was frequently He leak tested, in particular leak control was renewed at each change of gas cylinders. The room was under constant forced ventilation. The quantity of PH_3 used however was always far below the threshold limit value.[11]

PH_3, NO_2, CO_2, and SO_2 were supplied by Air Liquide, whereas Ar and N_2O came from UCAR(Union Carbide) and Praxair, respectively. The purity grades in the same order as the here above-mentioned gases were ≥99.999%, ≥99%, ≥99.998%, ≥99.98%, ≥99.9999%, and ≥99.998%.

III. Results and Discussion

A. Quenching of $PH_2(\tilde{A}^2A_1;\ v'_2 = 1,0)$. The photolysis of PH_3 by ArF laser 193 nm radiation produces PH_2 radicals in both $\tilde{A}^2A_1$ excited and $\tilde{X}^2B_1$ ground electronic states. The time evolution of $\tilde{A}^2A_1$ could thus have been studied by monitoring the emissions produced by the photolysis process, but for reasons of better selectivity of the vibrational levels to be investigated, LIF was preferred.

Time-resolved fluorescence curves were collected, and their mathematical treatment to obtain the decay parameters have been extensively reported in previous papers.[1]

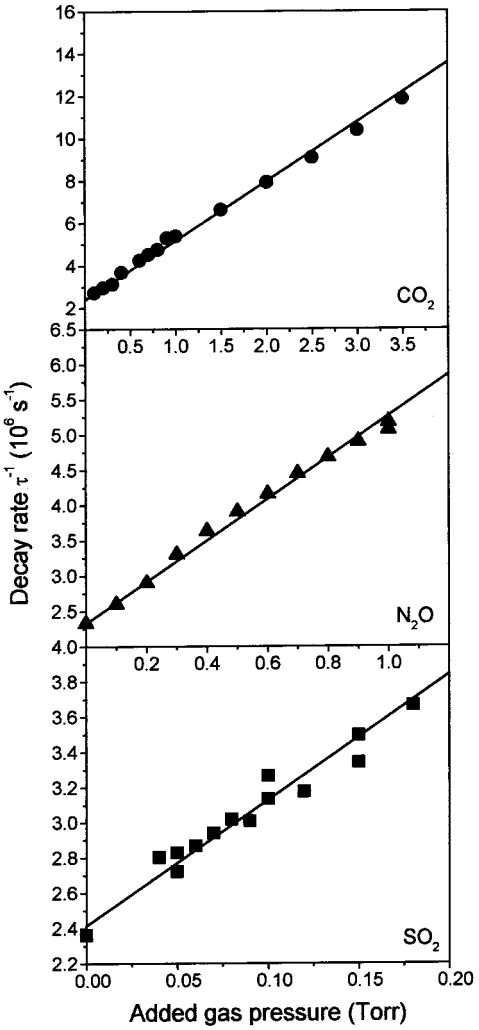

Figure 1. Quenching of $PH_2(\tilde{A}^2A_1;\ v'_2 = 1)$ by CO_2, N_2O, and SO_2. Plots of fluorescence decay rate τ^{-1} vs quencher pressure. Mixtures of added gas with 0.1 Torr PH_3 and 1 Torr Ar.

Briefly, it has been seen that the time variation of the $PH_2(\tilde{A}^2A_1;\ v'_2 = 1,0)$ fluorescence intensity in all circumstances follows the decay Stern−Volmer mechanism which is expressed by

$$\tau^{-1} = \tau_R{}^{-1} + k_D + k_{PH3}[PH_3] + k_{Ar}[Ar] + k_M[M] \quad (1)$$

where τ^{-1} is the decay rate of the fluorescence curve, τ_R is the radiative lifetime, k_D is the diffusion constant, and k_{PH3}, k_{Ar}, and k_M are the quenching constants produced by PH_3, Ar, and the added gas M, respectively.

In Figures 1 and 2, plots of τ^{-1} decay rates against quencher pressure are displayed.

The experimental data were fitted by weighted linear least-squares and the different k_M quenching constants obtained. These latter are shown in Table 1 together with all of the constants reported in previous papers. Confidence level errors of 95% are reported.

In analyzing $PH_2(\tilde{A}^2A_1;\ v'_2 = 1)$ quenching due to collisions with rare gases[3], it has been observed that the data follow quite well Parmenter and co-workers' theory[12] according to which

$$\ln \sigma = \beta(\epsilon_{MM}/k)^{1/2} + \ln C \quad (2)$$

TABLE 1: Quenching of $PH_2(\tilde{A}^2A_1;v'_2 = 1,0)$ by Triatomic Molecules,[a] Diatomic Molecules,[b] PH_3, and Rare Gases[c]

	$k_M \times 10^{11}$[d] (cm^3 molec.$^{-1}$ s^{-1})		σ[e] (Å^2)		$P = \sigma/\sigma_{hs}$[f] $\times 10^2$	
quencher M	$v'_2 = 1$	$v'_2 = 0$	$v'_2 = 1$	$v'_2 = 0$	$v'_2 = 1$	$v'_2 = 0$
CO_2	8.64 ± 0.43	2.96 ± 0.12	14.9 ± 0.7	5.12 ± 0.21	33.0	11.3
N_2O	9.07 ± 0.36	2.98 ± 0.11	15.7 ± 0.6	5.16 ± 0.19	35.8	11.8
SO_2	22.0 ± 2.9		40.9 ± 5.5		83.8	
H_2	5.79 ± 0.44	2.60 ± 0.10	3.17 ± 0.24	1.42 ± 0.03	9.50	4.28
N_2	5.05 ± 0.39	2.12 ± 0.10	7.82 ± 0.61	3.28 ± 0.11	18.8	7.90
CO	7.40 ± 0.62	3.44 ± 0.18	11.5 ± 1.0	5.33 ± 0.27	28.3	13.2
NO	19.6 ± 1.8	7.70 ± 0.35	30.9 ± 2.9	12.1 ± 0.6	78.2	30.8
PH_3	34.4 ± 3.3	24 ± 5	56.0 ± 5.4	39 ± 8	134	95
He	2.51 ± 0.22		1.88 ± 0.17		6.3	
Ne	2.03 ± 0.18		2.86 ± 0.25		8.9	
Ar	3.24 ± 0.11		5.49 ± 0.18		14.3	
Kr	3.78 ± 0.14		7.32 ± 0.27		18.0	
Xe	5.50 ± 0.41		11.2 ± 0.8		24.2	

[a] This work. [b] The data by diatomic molecules, PH_3, and rare gases come from previous works (see ref 1). [c] Rate constant k_M, cross section σ, and probability per collision P. [d] The data are reported with 95% confidence level errors. [e] The cross sections have been derived from k_M using the formula reported in Yardley, J. T. *Introduction to Molecular Energy Transfer*; Academic: New York, 1980; pp 16−19. The room temperature is 298 K. [f] To calculate the various hard sphere collision cross sections σ_{hs}, the diameter of PH_2 has been estimated as approximately equal to that of H_2S (see ref 1). The diameters of CO_2, N_2O, and SO_2 are taken from Khristenko, S. V.; Maslov, A. I.; Shelveko, V. P. *Molecules and Their Spectroscopic Properties*; Springer: Berlin, 1998.

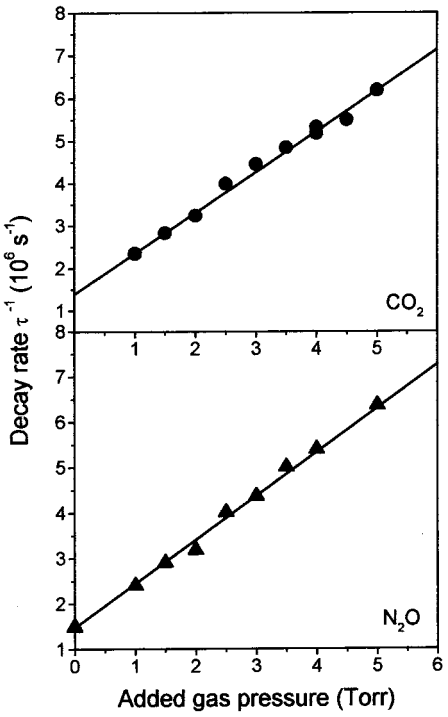

Figure 2. $PH_2(\tilde{A}^2A_1;\ v'_2 = 0)$ fluorescence decay rate τ^{-1} vs CO_2 and N_2O pressure. Mixtures with 0.1 Torr PH_3 and 1 Torr Ar.

where σ is the cross section of the quenching process,

$$\beta = (\epsilon'_{A^*A^*}/kT^2)^{1/2}$$

and

$$(\epsilon_{A^*A^*})^{1/2} = 0.6(\epsilon'_{A^*A^*})^{1/2}$$

$\epsilon_{A^*A^*}$ and ϵ_{MM} represent the A*−A* and M−M Lennard-Jones pair potential well depths, respectively. A* is the excited molecule, and M is the quencher. This means that ln σ is linearly dependent on $(\epsilon_{MM}/k)^{1/2}$. The removal mechanism of $PH_2(\tilde{A}^2A_1;\ v'_2 = 1)$ should be a transition to the underlying isoenergetic higher vibrational levels of the ground electronic state, possibly coupled with a simultaneous $v'_2 = 1 \rightarrow v'_2 = 0$ vibrational relaxation process. The latter should, however, be unimportant, if not negligible, as it has been experimentally seen in one of our previous works[5] that the $v'_2 = 4 \rightarrow v'_2 = 3$ collision-induced relaxation gives rise to a very weak $v'_2 = 3$ fluorescence.

When the quenching data of $(\tilde{A}^2A_1;\ v'_2 = 1)$ produced by diatomic quenchers H_2, N_2, CO, and NO are plotted in the same Parmenter's plot as those produced by rare gases,[1] a clear deviation in the trend of variation of ln σ with $(\epsilon_{MM}/k)^{1/2}$ is observed. This deviation is not caused by experimental fluctuations but rather by a systematic phenomenon as the data obtained for the quenching of $(\tilde{A}^2A_1;\ v'_2 = 0)$ by the same molecular quenchers behave in the same manner (see Figure 5 of ref 1 and Figure 4 in the following).

The quenching data of $v'_2 = 0$ by rare gases are not available, but it is presumable that they must show a parallelism similar to that observed with the diatomic quenchers and must be due to the same quenching mechanism as $v'_2 = 1$.

The deviation shown by both $v'_2 = 1$ and′ 0 data of H_2, N_2, CO, and NO from those of the rare gases are likely due to a second channel of removal which should be active in parallel to the above-mentioned transitions of the excited PH_2 vibronic species to the underlying isoenergetic vibrational levels of the ground electronic state.[1]

As there seems to be a correlation between the magnitude of the deviations and the vibrational frequencies of the diatomic quenchers, this additional channel has been assumed to be due to an intermolecular E−V process.[1]

The difference between the quenching data of the two $v'_2 =$ 1 and 0 vibrational levels may partly be explained by the difference in density of states of the ground electronic state at the same energies of these levels.

Figure 3 shows the Parmenter's plot of the $PH_2(\tilde{A}^2A_1;\ v'_2 =$ 1) quenching data of CO_2, N_2O, and SO_2 together with those of the rare gases, diatomic molecules, and PH_3. Again, these tri- and tetra-atomic molecules do not follow the trend delineated by the rare gases.

Figure 4 represents the quenching data by diatomic and triatomic molecules and PH_3 for both $v'_2 = 1$ and′ 0. As can be seen, the above-mentioned paralleslism between the two sets of data extends to more complex molecules. The SO_2 data of

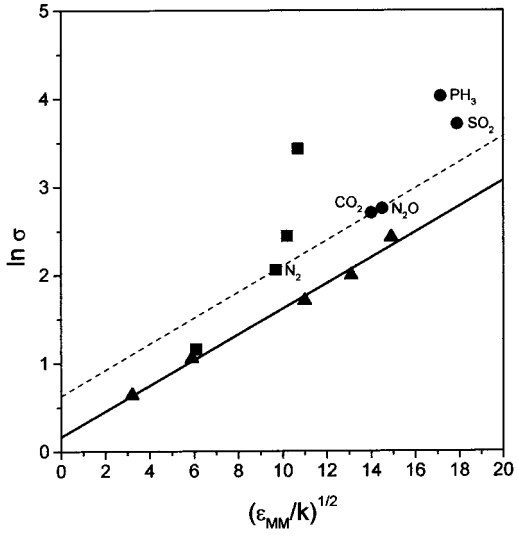

Figure 3. Parmenter's plot for $PH_2(\tilde{A}^2A_1; v'_2 = 1)$ quenching. (▲), rare gas data; (■), quenching by H_2, N_2, CO, and NO with increasing $(\epsilon_{MM}/k)^{1/2}$ values; (●), data by the indicated molecules. $(\epsilon_{MM}/k)^{1/2}$ are taken from ref 12, except that of PH_3 which has been evaluated (see ref 1). Solid line: linear fit of rare gas data. Dashed line: linear fit of N_2, CO_2 and N_2O data.

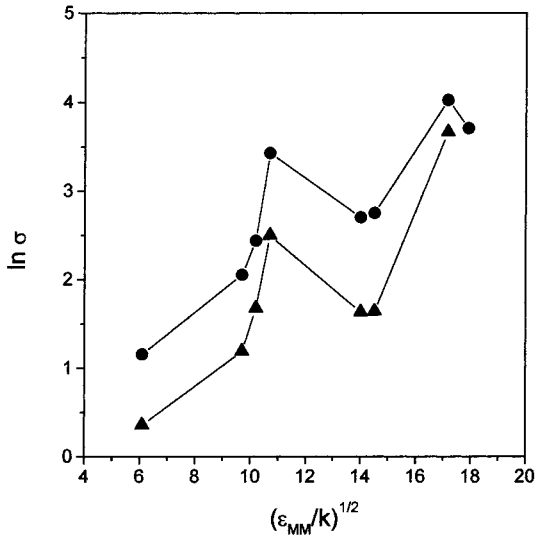

Figure 4. Parmenter's plots for $PH_2(\tilde{A}^2A_1; v'_2 = 1$ and 0) quenching by H_2, N_2, CO, NO, CO_2, N_2O, PH_3, and SO_2 with increasing $(\epsilon_{MM}/k)^{1/2}$ values. (●), $v'_2 = 1$ data; (▲), $v'_2 = 0$ data.

$v'_2 = 0$ is lacking for serious trouble with the experimental setup, but there is no doubt that it should follow the trend shown in $v'_2 = 1$.

From Figure 4, it can be seen that the decrease of quenching efficiency from NO to CO_2 and N_2O is real.

The solid line in Figure 3, obtained from a least-squares fitting of the quenching data of $v'_2 = 1$ by rare gases can reasonably be considered as representing the pure mechanism of removal by collision-induced transition to the isoenergetic underlying vibrational levels of the ground electronic state. It is expressed by

$$\ln \sigma = 0.145(\epsilon_{MM}/k)^{1/2} + 0.162 \qquad (3)$$

from which the cross section of the quenching part presumably produced by this mechanism could be calculated for each of the molecular quenchers under investigation by substitution of $(\epsilon_{MM}/k)^{1/2}$ in eq 3 with their respective values.

TABLE 2: Comparison of the Experimental $PH_2(\tilde{A}^2A_1; v'_2 = 1)$ Quenching Cross Sections, σ_{exp}, with the Cross Sections Deduced from the Fitting Line of the Rare Gas Data in the Parmenter's Plot,[a] σ_{calc}

quencher M	$(\epsilon/k)^{1/2}$ ($K^{1/2}$)	σ_{exp} (Å^2)	σ_{calc} (Å^2)	$\Delta\sigma$	$\Delta\sigma/\sigma_{calc}$
H_2	6.1	3.17	2.85	0.32	0.11
N_2	9.7	7.82	4.81	3.01	0.63
CO	10.2	11.5	5.17	6.33	1.22
NO	10.7	30.9	5.56	25.34	4.56
CO_2	14	14.9	8.98	5.92	0.66
N_2O	14.5	15.7	9.66	6.04	0.63
SO_2	17.9	40.9	15.83	25.07	1.58
PH_3	17.15	56.0	14.20	41.8	2.94

[a] The $(\epsilon_{MM}/k)^{1/2}$ values are taken from refs 12 and 1.

Table 2 reports these calculated cross sections, the experimental ones, their differences $\Delta\sigma$, and the ratios of these differences to the calculated values.

From the $\Delta\sigma/\sigma_{calc}$ values, one might divide the quenchers in three groups, one with $\Delta\sigma$ decidedly larger than σ_{calc}, i.e., NO, SO_2, and PH_3, another with $\Delta\sigma < \sigma_{calc}$, i.e., N_2, N_2O, and CO_2, and a third with CO which seems to represent a transiton between the first two groups having $\Delta\sigma \cong \sigma_{calc}$.

According to the discussion concerning the diatomic quenchers, NO is presumably also involved in a purely physical collision-induced intermolecular E−V energy transfer process with $PH_2(\tilde{A}^2A_1; v'_2 = 1,0)$. As it is however known from ref 2 that NO reacts chemically with $PH_2(\tilde{X}^2B_1; v''_2 = 0,1)$ ground eletronic species giving rise very probably to $PN + H_2O$ through the formation of an adduct, a similar chemical reactivity has also to be considered in the quenching process which would further justify the high efficiency of NO.

As to SO_2 and PH_3, a collisional E−V energy exchange with $PH_2(\tilde{A}^2A_1; v'_2 = 1)$ cannot by itself explain neither their $\Delta\sigma/\sigma_{calc}$ values nor, by comparing the different vibrational frequencies available, the large difference in quenching efficiency between them and N_2O and CO_2. Some chemical reactivity also has again to be invoked. If a metathesis reaction between $PH_2(\tilde{A}^2A_1)$ and PH_3 might occur, thermochemical considerations rule out direct reactions for SO_2. A long-lived adduct formation mechanism may however be proposed:

$$PH_2^* + M \rightarrow [PH_2{\cdot}M]^* \rightarrow PH_2(\tilde{X}^2B_1; v''_2) + M\dagger \qquad (4)$$

where PH_2^* stands for $PH_2(\tilde{A}^2A_1; v'_2)$, $[PH_2{\cdot}M]^*$ stands for the excited adduct, M stands for PH_3 or SO_2, and M† represents the ground or excited vibrational species. As a consequence of a redistribution of the excitation energy $(\tilde{A}^2A_1)$ of PH_2 among the various degrees of freedom of the intermediate compound the PH_2 electronic excitation is removed in the back redissociation of the latter.

All of the quenching processes so far mentioned are present in this mechanism with the difference that they occur here through the formation of an adduct which is a chemical entity and which could be stabilized under certain pressure conditions. The mechanism[4] represents thus what might be called "chemical" quenching processes, whereas the collision-induced ones are physical.

A combination of all of these chemical and physical mechanisms would then result in the measured cross sections.

Whereas for NO, SO_2, and PH_3 the chemical channel appears to prevail over the physical one, for CO with $\Delta\sigma/\sigma_{calc} = 1.2$, there would exist a balance between the two. This means that for CO the formation of an adduct has also to be considered, even if this one should be more loosely bound. Such an adduct

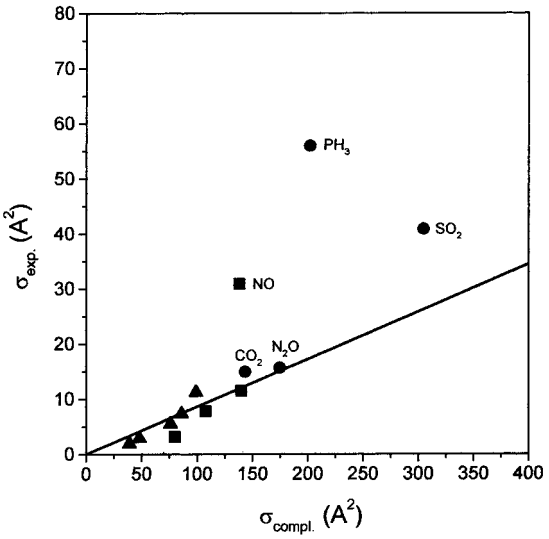

Figure 5. Plot of the measured quenching cross sections (σ_{exp}) of $PH_2(\tilde{A}^2A_1;\ v'_2 = 1)$ vs maximum quenching cross sections (σ_{compl}) calculated according to the collision complex formation model. (▲), rare gas data; (■), H_2, N_2, NO, and CO data in this order from left to right of the σ_{compl} axis; (●), data by the indicated molecules.

has been demonstated to exist for $CO + PH_2^+$.[13,14] It will be seen below that the adduct mechanism has also to be invoked to explain the large difference between CO and N_2 in deactivating $PH_2(\tilde{X};\ v''_2 = 1)$.

The $\Delta\sigma/\sigma_{calc}$ values are approximately 0.6 for N_2, N_2O, and CO_2. The dashed line drawn in Figure 3 through these quenchers (slope $\beta = 0.147$) is practically parallel to the Parmenter's line of the rare gas data ($\beta = 0.145$) showing that the quenching mechanisms of the three molecules should be the same but different from that of the rare gases. As it is rather difficult to think of an adduct between N_2 and PH_2, the quenching efficiency enhancement of N_2 with respect to the rare gas trend should essentially be due to a collision-induced process. The same has then to be said of the other two quenchers. The forementioned parallelism does not seem fortuitous as it is also observed for $PH_2(\tilde{A}^2A_1;\ v'_2 = 0)$ (see Figure 4).

Figure 5 reports a plot of the quenching data of $PH_2(\tilde{A}^2A_1;\ v'_2 = 1)$ against σ_{compl} calculated according to the collision complex formation theory.[15]

A short-lived complex of rather physical nature is supposed to be formed between the excited particle and the quencher in all collisions with impact parameters smaller than a certain value b_0 which corresponds to a balance between the collision kinetic energy E and the maximum of the long-range effective potential $V(r)$. This potential is the sum of attractive multipole interactions (dipole−dipole, dipole−quadrupole, dipole−induced dipole, and dispersion) and a centrifugal barrier Eb^2/r^2.[1,15] b_0 thus represents the maximum impact parameter for which mutual capturing of the collision partners at a certain E is possible, and gives rise to the capture cross section $\sigma_{cap}(E) = \pi b_0(E)^2$. During the brief existence of the complex, a redistribution of the total energy among the various degrees of freedom occurs resulting, at its redissociation, in the quenching of a certain amount of the excited species. The quenching cross section should thus be proportional to the capture cross section $\sigma_{cap}(E)$ which represents then its upper limit at the kinetic energy E. The thermal averaged capture cross sections have been calculated for all of the quenchers studied and are represented by σ_{compl} in Figure 5.

With the exception of NO, SO_2, and PH_3, the quenching data of the other molecules lie quite well on the straight line showing the above-mentioned proportionality. Their deactivation processes should then come from a collision complex formation, whereas with the other three molecules $PH_2(\tilde{A}^2A_1;\ v'_2 = 1)$ should be removed by mechanisms of different nature confirming what has already been found with the Parmenter's plot. It is surprising to see such a clear separation of the behavior of CO_2 and N_2O from that of SO_2.

The quenching data have also been compared with the cross sections calculated according to the Thayer and Yardley's dipole−dipole interaction theory.[16] The deviations of the molecular quenchers with respect to the rare gases found in the Parmenter's plot are again observed which however can be less easily quantified as the experimental data enter in the determination of some parameters of the Thayer and Yardley's formulas. The peculiar situations of NO and PH_3 seem here noticeably amplified denoting the different nature of their interaction mechanisms with $PH_2(\tilde{A}^2A_1;\ v'_2 = 1)$.

The three theories applied result thus to be complementary for the comprehension of the mechanisms involved by the studied added gases in the quenching of $PH_2(\tilde{A}^2A_1;\ v'_2)$.

For what concerns in particular the three triatomic quenchers, N_2O and CO_2 seem to interact with $PH_2(\tilde{A}^2A_1;\ v'_2)$ with the same mechanism as N_2, whereas a chemical activity has to be invoked for SO_2.

All of the above discussion, and in particular that of the Parmenter's plot, clearly is meant only to be an attempt to give a qualitative interpretation of the observed data. The effective roles played by the different mentioned mechanisms, physical and chemical, can only be ascertained by detailed quantum mechanical calculations which however are not available.

B. Vibrational Relaxation of $PH_2(\tilde{X}^2B_1;\ v''_2 = 1)$. In the photolysis of PH_3 by the 193 nm photons, $PH_2(\tilde{X}^2B_1)$ is produced in vibrationally excited states with $v''_2 > 3$.[1,17] $v''_2 = 1$ is then populated by subsequent relaxation from the upper states.

The kinetics of vibrational deactivation of $PH_2(\tilde{X}^2B_1;\ v''_2 = 1)$ was investigated by monitoring the time variation of their concentrations after the photolysis flash. This was done recording at various moments the total fluorescence induced by laser excitation of the $v'_2 = 1 \leftarrow v''_2 = 1$ transition.

All of the LIF curves thus obtained have been seen to vary with time according to an equation of the form

$$I(t) = C[\exp(-At) - \exp(-Bt)] \qquad (5)$$

which represents the typical kinetics of the lower state having zero population at $t = 0$ of a two-level system characterized by the two decay rates A and B. A refers to the lower level, and B refers to the higher one. During the evolution of the system, the lower level is populated by the upper one. C is a coefficient. Graphically, the fluorescence intensity rises to a maximum and then decays.

In designating the bulk of the higher bending vibrational levels of the PH_2 ground electronic state species formed in the photolysis process with $PH_2^\dagger$, a kinetic scheme concerning the time evolution of the $PH_2(\tilde{X}^2B_1;\ v''_2 = 1)$ concentrations can be set up. It has been reported in detail in previous papers[1], so it is presented here only in a condensed form:

$$PH_2^\dagger + M \rightarrow \text{products}$$

$$PH_2^\dagger + M \rightarrow PH_2(v''_2 = 1) + M$$

$$PH_2(v''_2 = 1) + M \rightarrow \text{products}$$

$$PH_2(v''_2 = 1) + M \rightarrow PH_2(v''_2 = 0) + M$$

where M is the added gas. It is clear that the complete scheme must include the same reactions with PH_3 and argon (with the buffer gas Ar the reactions giving rise to products are removed) instead of M.

The variation of ($v''_2 = 1$) concentrations with time

$$[PH_2(v''_2 = 1)] = [PH_2^{\dagger}]_0\{K/(K2 - K1)\}(-e^{-K2t} + e^{-K1t}) \quad (6)$$

has been derived by imposing, in compliance with eq 5, [($v''_2 = 1$)] = 0 at $t = 0$. This last condition further confirms what has been mentioned above concerning the $PH_2(\tilde{X}^2B_1;\ v''_2)$ production mechanism by ArF laser photolysis of PH_3. *K* is a constant which takes into account the relaxation of $PH_2^{\dagger}$ to $v''_2 = 1$ due to collisions with M, PH_3, and Ar, whereas K2 and K1 represent the total decay rates of $PH_2^{\dagger}$ and $v''_2 = 1$, respectively. The detailed expressions for K1 and K2 have been reported in previous works[1].

Briefly K1, which is here the more important of the two as it concerns the kinetics of $v''_2 = 1$ removal, is seen to be a linear function of [M]:

$$K1 = a[M] + b \quad (7)$$

where *a* is the sum of the collision-induced relaxation constant and the constant of a possible chemical reaction of $PH_2(v''_2 = 1)$ with M and *b* is the total removal rate produced by the background gases (0.1 Torr PH_3 + 1 Torr Ar).

As the rising part of the LIF curves present, most of the time, poor statistics, only the decay branch has been used to derive the K1 rates.

Figure 6 plots K1 against the pressure of CO_2, N_2O, and SO_2, which stand here for the added gas M.

Coefficient *a* of eq 7 can thus be derived from the slopes of the fitting lines.

Experiments of $PH_2(\tilde{X}^2B_1;\ v''_2 = 0)$ removal in the presence of N_2O and CO_2 have been carried out in order to see whether PH_2 reacts chemically with these compounds and possibly measure the reactive constants. No reaction happened. Experiments have not been performed with SO_2, but the enthalpy value of the reaction leading to the formation of PS + 2OH is +94 kcalmol^{-1}, i.e., the reaction is strongly endothermic.

The above determined *a* coefficients must therefore be considered as being due only to deactivation of $v''_2 = 1$.

They are reported with 95% confidence level errors in Table 3 together with those of PH_3, rare gases, and diatomic quenchers determined in previous papers[1].

If all of these data are plotted against $\mu^{1/2}$, the square root of the reduced mass of the respective collision pairs, according to SSH theory[4] for V−T relaxation, the anomalously large deactivation efficiencies of the three triatomic molecules and PH_3, compared to those of the rare gases and the diatomic molecules except NO, can immediately be noticed.

This state of things cannot be explained by chemical activity between $PH_2(\tilde{X}^2B_1;\ v''_2 = 1)$ and N_2O, CO_2, and SO_2, as it has experimentally been found above that $PH_2(\tilde{X}^2B_1)$ does not react chemically with these molecules. It must therefore be due to some other mechanism, different from the V−R,T one so far proposed for the other quenchers[1] and also from a simple V−T process.

On the other hand, the higher efficiency of N_2O (by a factor of 2.3) compared to CO_2 of equal mass has also to be explained.

Table 4 shows the frequencies of the different normal vibrations of N_2O, CO_2, SO_2, and PH_3. It can be seen that all these molecules have a vibration close to that of $PH_2(\tilde{X}^2B_1;\ v''_2 = 1)$ which is 1102 cm^{-1}. The differences of these vibrations with $v''_2 = 1$, $\Delta\nu$, are also reported.

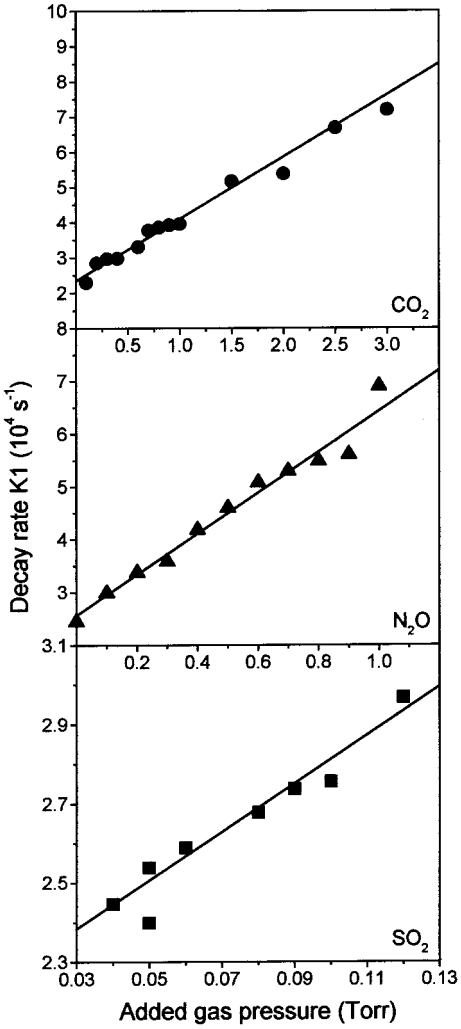

Figure 6. $PH_2(\tilde{X}^2B_1;\ v''_2 = 1)$ LIF curve decay rate K1 vs CO_2, N_2O, and SO_2 pressure. Mixtures with 0.1 Torr PH_3 and 1 Torr Ar.

TABLE 3: Collision-Induced Removal of $PH_2(\tilde{X}^2B_1;\ v''_2 = 1)$[a]

quencher M	$\mu^{1/2}$	$k_M \times 10^{14}$[b] (cm^3 molec.$^{-1}$ s^{-1})	$\sigma \times 10^3$ (Å^2)	$P = \sigma/\sigma_{hs} \times 10^4$
CO_2	4.34	54.4± 6.6	94.0± 11.5	20.8
N_2O	4.34	119 ± 11	206 ± 19	47.1
SO_2	4.67	189 ± 42	350 ± 79	71.9
H_2	1.38	58.4 ± 1.2	32.0 ± 6.4	9.6
N_2	3.89	5.09 ± 0.44	7.89 ± 0.69	1.9
CO	3.89	15.9 ± 2.1	24.6 ± 3.2	6.1
NO	3.96	668 ± 157	1054 ± 248	269
PH_3	4.09	456 ± 37	743 ± 60	183
He	1.89	9.77 ± 1.66	7.34 ± 1.24	2.44
Ne	3.54	6.26 ± 0.70	8.82 ± 0.99	2.75
Ar	4.25	6.70 ± 1.37	11.3 ± 2.3	2.95
Kr	4.87	7.65 ± 1.71	14.8 ± 3.3	3.65

[a] The data for triatomic quenchers are obtained in this work, whereas those of the other quenchers come from previous papers (see ref 1). Reduced mass of the collision pair $\mu^{1/2}$, rate constant k_M, cross section σ, and probability per collision P. The cross sections have been derived from k_M using the formula given in J. T. Yardley *op. cit.*, pp 16−19. The room temperature is 298 K. [b] 95% confidence level errors are reported.

TABLE 4: Normal Vibration Frequencies of $PH_2(\tilde{X}^2B_1)$ and the Polyatomic quenchers[a] under Study[b]

	ν_1 (cm^{-1})	ν_2 (cm^{-1})	ν_3 (cm^{-1})	ν_4 (cm^{-1})	$\Delta\nu = \nu_{PH2} - \nu_n$ (cm^{-1})	$P = \sigma/\sigma_{hs} \times 10^4$
PH_2		1102				
PH_3	2322.9	992.0	2327.7	1122.4	$n = 4$ −20.4	183
SO_2	1151.3	517.6	1361.7		$n = 1$ −49.3	71.9
N_2O	2223.8	588.8	1284.9		$n = 3$ −182.9	47.1
CO_2	1388.2	667.4	2349.2		$n = 1$ −286.2	20.8

[a] Taken from Herzberg, G. *Molecular Spectra and Molecular Structure III. Electronic Spectra and Electronic Structure of Polyatomic Molecules*; D. Van Nostrand: Princeton, New Jersey, 1967. [b] Minimum frequency mismatch $\nu_{PH2} - \nu_n$ between the vibrations of PH_2 and the quenchers.

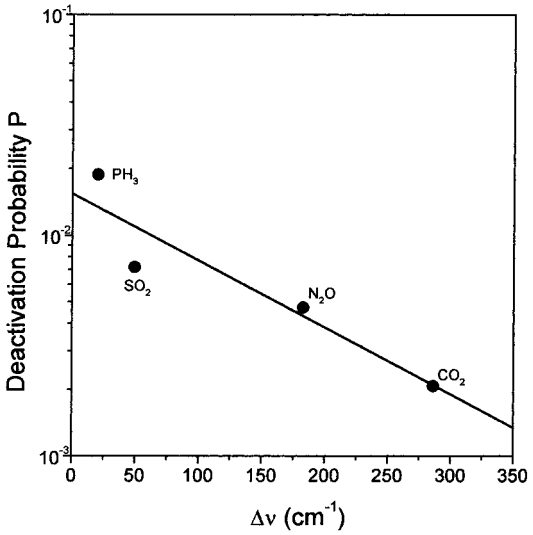

Figure 7. Deactivation probability of $PH_2(\tilde{X}^2B_1; v''_2 = 1)$ vs $\Delta\nu$.

The mechanism responsible for the deactivation of $v''_2 = 1$ must therefore be an endothermic intermolecular V−V energy transfer:

$$PH_2(\tilde{X}^2B_1; v''_2 = 1) + M(v = 0) \rightarrow PH_2(\tilde{X}^2B_1; v''_2 = 0) + M(v = 1) \quad \Delta E > 0 \quad (8)$$

involving in each quencher M the vibration with the closest frequency to ν_2 of $PH_2(\tilde{X}^2B_1)$. This will explain all of the questions raised above.

According to the semilog plot of Figure 7, the dependence of energy transfer probability on the $\Delta\nu$ energy mismatch appears to be linear, following somehow the SSH−Tanczos behavior.[20]

By using the principle of detailed balance, the probability of occurrence of the exothermic reactions $PH_2(\tilde{X}^2B_1; v''_2 = 0) + M(v = 1)$ have also been calculated. A linear plot similar to that of Figure 7 has been obtained.

These calculated data are much higher than those, reported by Callear,[18] due to short-range interactions which, in fact, usually give rise to transfer probabilities lower than 10^{-3}.

According to a simplified theory for nonresonant V−V relaxation due to long-range forces reported by Yardley,[19] $\ln P$ should vary linearly with $\Delta\nu^{2/3}$. By plotting our data against $\Delta\nu^{2/3}$, a linear plot has effectively been obtained. Thus the relaxation of $PH_2(\tilde{X}^2B_1; v''_2 = 1)$ induced by CO_2, N_2O, SO_2, and PH_3 seems to be due to long-range interactions.

An attempt to plot the data according to Parmenter's theory has also been done, but a convincing linear correlation with $(\epsilon_{MM}/k)^{1/2}$ has not been observed. Besides, the linear fit gives a β value larger than that derived from the relaxation of $PH_2(\tilde{X}^2B_1; v''_2 = 1)$ by the rare gases[3] by a factor of 6.4, whereas it should give the same value because both data sets refer to the same excited species. One of the conditions for the applicability of Parmenter's theory is that resonance effects must be absent between the collision partners. Strictly speaking, we are here not in the presence of resonant energy exchanges between $PH_2(v''_2 = 1)$ and the above quenchers as $\Delta\nu$ varies between 20.4 and 286.2 cm^{-1}, but we may perhaps be at the limit of its applicability.

The deactivation constant of $PH_2(v''_2 = 1)$ by CO is factor 3.2 higher than that produced by N_2 of the same mass. As discussed in ref 1, this large difference cannot be explained neither by the dipole moment of CO which is rather weak, 0.1 D, nor by the difference in polarizability, 1.95 $Å^3$ for CO and 1.76 $Å^3$ for N_2. Besides, CO and N_2 should deactivate $v''_2 = 1$ through an intramolecular V−R,T mechanism,[1] so the difference in energy mismatch between $v''_2 = 1$ and CO ($\Delta\nu = 1067$ cm^{-1}) on one hand, and between $v''_2 = 1$ and N_2 ($\Delta\nu = 1256$ cm^{-1}) on the other, which can be important in a V−V process, is of little help in this context. The formation of an adduct between $PH_2(\tilde{X}; v''_2 = 1)$ and CO, and its subsequent re-dissociation to $PH_2(\tilde{X}; v''_2 = 0)$ + CO, according to a similar mechanism already invoked in the quenching of $PH_2(\tilde{A}; v'_2 = 1)$ by CO, seems to be a possible channel which can account for these different efficiencies. Apart from the above-mentioned experimental demonstration of the existence of the adduct $CO\cdot PH_2^+$,[13,14] Essefar et al.[20] have studied the potential energy surfaces of the reaction CO + PH_2^+ and shown that the formation of the adduct is an exothermic process. The extension of the possibility of an adduct formation between PH_2 and CO appears thus not so improbable.

IV. Conclusion

Each of the three theories we have used to treat the quenching data of $PH_2(\tilde{A}^2A_1; v'_2 = 1)$ produced by the three triatomic quenchers studied in this work seems to give a different insight into their interaction mechanism.

With the complex formation model, CO_2 and N_2O appears to belong to the same group of the rare gases, H_2, N_2, and CO, whereas SO_2 presents the anomalous situation of NO and PH_3. The Thayer and Yardley's theory also puts the same former molecules in one cluster but shows deviations of N_2, CO, CO_2, and N_2O from the rare gas and H_2 behavior. Whereas the anomaly of NO and PH_3 seems to be amplified, the SO_2 data appears justified. This latter fact is due to the use of the limited number of experimental data in the calculation of the parameters of Thayer and Yardley's formulas. With Parmenter's theory, a somehow more quantitative estimation of the deviations of these triatomic quenchers from the rare gas trend, as well as that of the previously observed deviations of the diatomic ones, can be made. Some idea about their interaction mechanism can then be put forward. CO_2 and N_2O seem to behave as N_2, whereas a chemical reactivity would also be responsible for the effect of SO_2. Further investigations with other triatomic and more complex molecules will be carried out, as soon as our apparatus will permit it, to have more information about the quenching mechanisms and possibly confirm the tendency of CO_2, N_2O, and N_2.

More work will also be done for the V−V energy transfer between $PH_2(v''_2 = 1)$ and the quenchers using molecules with different $\Delta\nu$ in order to cover a wider range of frequency mismatches.

References and Notes

(1) Nguyen Xuan, C.; Margani, A. *J. Chem. Phys.* **1998**, *109*, 9417 and references therein.
(2) Nguyen Xuan, C.; Margani, A.*Chem. Phys. Lett.* **2000**, *321*, 328.
(3) Nguyen Xuan, C.; Margani, A.; Mastropietro, M. *J. Chem. Phys.* **1997**, *106*, 8473.
(4) Schwartz, R. N.; Slawsky, Z. J.; Herzfeld, K. H. *J. Chem. Phys.* **1952**, *20*, 1591.
(5) Nguyen Xuan, C.; Margani, A. *J. Chem. Phys.* **1990**, *93*, 136.
(6) Nguyen Xuan, C.; Margani, A. unpublished data.
(7) Melville, H. W. *Proc. R. Soc. London, Ser. A* **1933**, *139*, 541.
(8) Norrish, R. G. W.; Oldershaw, G. A. *Proc. R. Soc. London, Ser. A* **1961**, *262*, 10.
(9) Ridgway, S. T.; Wallace, L.; Smith, G. R. *Astrophys. J.* **1976**, *207*, 1002.
(10) Stringfellow, G. B. *Organometallic Vapor-Phase Epitaxy: Theory and Practice*; Academic: New York, 1989.
(11) L'Air Liquide. *Encyclopédie des Gas*; Elsevier: Amsterdam, The Netherlands, 1976.
(12) Lin, H. M.; Seaver, M.; Tang, K. Y.; Knight, A. E. W.; Parmenter, C. S. *J. Chem. Phys.* **1979**, *70*, 5442.
(13) Smith, D.; McIntosh, B. J.; Adams, N. G. *J. Chem. Phys.* **1989**, *90*, 6213.
(14) Adams, N. G.; McIntosh, B. J.; Smith, D. *Astron. Astrophys.* **1990**, *232*, 443.
(15) Holtermann, D. L.; Lee, E. K. C.; Nanes, R. *J. Chem. Phys.* **1982**, *77*, 5327.
(16) Thayer, C. A.; Yardley, J. T. *J. Chem. Phys.* **1972**, *57*, 3992.
(17) Koplitz, B.; Xu, Z.; Baugh, D.; Buelow, S.; Häusler, D.; Rice, J.; Reisler, H.; Qian, C. X. W.; Noble, M.; Wittig, C. *Faraday Discuss. Chem. Soc.* **1986**, *82*, 125.
(18) Callear, A. *Appl. Opt. Suppl.* **1965**, *2*, 145.
(19) Yardley, J. T. *Introduction to Molecular Energy Transfer*; Academic: New York, 1980; pp 151−152.
(20) Tanczos, F. I. *J. Chem. Phys.* **1956**, *25*, 439.
(21) Essefar, M.; Luna, A.; Mó, O.; Yáñez, M. *Chem. Phys. Lett*. **1994**, *223*, 240.